

Optimizing Cooperative Video Streaming in Wireless Networks

Zhangyu Guan^{†‡}, Tommaso Melodia[†], and Dongfeng Yuan[†]

[†]Department of Electrical Engineering, University at Buffalo, The State University of New York, Buffalo, NY, 14260

[‡]School of Information Science and Engineering, Shandong University, China, 250100

Email: zhangyuguan@sdu.edu.cn, tmelodia@buffalo.edu, dfyuan@sdu.edu.cn

Abstract—Physical-layer cooperation allows leveraging the spatial diversity of the wireless channel without requiring multiple antennas on a single device. However, most research in this field focuses on optimizing physical layer metrics, with little consideration for network-wide and application-specific performance measures. This paper studies cross-layer design techniques for video streaming over cooperative networks. The problem of joint video rate control, relay selection, and power allocation is formulated as a mixed-integer nonlinear problem, with the objective of maximizing the sum peak signal-to-noise ratio (PSNR) of a set of concurrent video sessions. An asynchronous, distributed and localized low-complexity algorithm is designed, based on the iterative solution of convex optimization problems at each individual node. In addition, a global-optimization centralized algorithm based on convex relaxations of non-convex constraints is also proposed as performance benchmark. The distributed algorithm is shown to achieve performance within a few percentage points of the optimal solution. It is also shown that cooperative relaying allows nodes to reduce the overall power consumption without leading to a perceivable decrease in video quality.

I. INTRODUCTION

The *spatial diversity* of the wireless channel can be leveraged to improve the performance of a communication link by using multiple transceiver antennas to effectively cope with fading. The underlying principle is that different propagation channels can be established with multiple transceiver pairs between a transmitting and a receiving node. By sending signals that carry the same information through different channels, multiple faded copies of the same information can be obtained at the receiving node. The communication link reliability can then be considerably improved since, intuitively, the probability that all channels go down at the same time is low, resulting in higher data rate or lower power consumption.

Spatial diversity is traditionally exploited by using multiple transceiver antennas (i.e., *multiple input multiple output* (MIMO) [1]). However, equipping a mobile device with multiple antennas may not be practical, since the minimum required separation between the antennas is dictated by the operating radio wavelength. The concept of *cooperative communications* has been therefore proposed to achieve spatial diversity

This research was carried out while Zhangyu Guan was a visiting scholar at the State University of New York at Buffalo. The work of Zhangyu Guan and Dongfeng Yuan was supported by the NSFC (No. 60832008, No. 61071122). The work of Tommaso Melodia was supported in part by the National Science Foundation under grant CNS-1055945.

without requiring multiple transceiver antennas on the same node [2], [3]. In cooperative communications, in their *virtual multiple-input single-output* (VMISO) variant, each node is equipped with a single antenna, and relies on the antennas of neighboring devices to achieve spatial diversity. There is a vast and growing literature on information and communication theoretic results in cooperative communications. The reader is referred to [4], [5] and references therein for excellent surveys of the main results in this area. However, the common objective of most research in this field is to optimize physical layer performance measures (i.e., bit error rate and link outage probability), without considering in much detail how cooperation interacts with higher layers of the protocol stack to improve network performance measures. For example, [6], [7] investigate the achievable rates and diversity gains of cooperative schemes focusing on a single source and destination pair. Some initial promising work on networking aspects of cooperative communications includes studies on medium access control protocols to leverage cooperation [3], [8], cooperative routing [9], [10], optimal network-wide relay selection [11], [12], and optimal stochastic control [13]. Most recently, the impact of cooperative relaying on network throughput was also investigated in conjunction with other advanced communication techniques, i.e., cognitive radio (CR) [14], [15] and network coding [16]. However, none of these works considers the impact of cooperation on end-to-end video delivery. Moreover, in most cases, these works assume an interference-free network, i.e., orthogonal channels have been established a-priori.

This paper studies cross-layer design techniques for video streaming over cooperative wireless networks with distributed control. Specifically, we study strategies for joint control of the video encoding rate at the application layer, relay selection, and power control at the link and physical layers, to maximize the sum peak signal-to-noise ratio (PSNR) of multiple concurrent video sessions. It is worth pointing out that relay selection in cooperative communications is different from traditional routing. In cooperative communications, transmission is carried out over two time-slots [2]. In the first time-slot, the source node broadcasts a signal to both the destination and relay nodes. Then, in the second time-slot, the relay node processes and then forwards the received signal to the destination node. Hence, the destination node receives two

copies of the original signal and decodes them *jointly* using maximal ratio combining [2]. In traditional routing, a relay node simply forwards packets received from previous hops without any processing. The main contributions of this paper are as follows:

- 1) We first formulate the problem of *joint rate control, relay selection, and power control for video streaming in cooperative networks* as a non-convex and combinatorial optimization problem (i.e., a mixed-integer non-linear problem (MINLP)). The problem is in general NP-hard [17] and cannot be solved efficiently through conventional optimization techniques.
- 2) We propose and study an asynchronous, distributed and localized low-complexity solution algorithm based on the iterative solution of convex optimization problems at each individual node.
- 3) We develop a globally optimal solution algorithm with provable convergence based on convex relaxations of non-convex problem constraints. By applying the resulting algorithm to instances of interest, we show that *cooperative relaying allows reducing the overall power consumption without leading to a perceivable decrease in video quality*.
- 4) We compare the performance of the distributed algorithm with the optimal algorithm and show its excellent video quality performance.

The rest of the paper is organized as follows. In Section II, we briefly describe the communication system model and introduce the problem formulation. The distributed algorithm is described in Section III, while the centralized algorithm is then discussed in Section IV. Examples and numerical results are discussed in Section V. Finally, we draw the main conclusions in Section VI.

II. PROBLEM FORMULATION

We consider a decentralized video streaming network, where each source node compresses a video sequence at a given rate. The scenario considered could be for example representative of a multimedia sensor network [18]. The video content is enqueued at the source node buffer and then transmitted to the destination through a direct or cooperative link. If the video packet is not received before a predefined play-out deadline, the packet is dropped. Video packets can also be dropped because of transmission errors caused by interference or channel fading. Cooperative communication techniques are employed on each link to potentially increase the channel capacity. There are multiple potential relay nodes, and each video session can select one of them as a relay node.

There are two common cooperation strategies: amplify-and-forward (AF) and decode-and-forward (DF) [2]. In AF, the relay simply amplifies the received signal and forwards it to the destination. With DF, the relay first decodes the received signal, then forwards it if it can be successfully decoded. In this paper, we concentrate on the DF strategy. However, our results can be extended to AF. The objective of the problem is to maximize the sum of the video qualities (expressed as the

sum PSNR) of multiple concurrent video sessions, by jointly regulating the video encoding rate for each session, adjusting the transmission power for each source and relay node, and selecting the optimal relay node for each session. We start by introducing the link capacity model for direct transmission and for cooperative relaying, and the video distortion model in Section II-A. Then, in Section II-B we formulate the MINLP problem.

A. Link Capacity and Video Distortion Model

Denote \mathcal{S} as the set of video sessions, and \mathcal{R} as the set of potential relay nodes. Define the vector of relay assignments as $\alpha = \{\alpha_{s,r} | s \in \mathcal{S}, r \in \mathcal{R}\}$, where $\alpha_{s,r} = 1$ iff relay node r is selected as relay for video session s , and $\alpha_{s,r} = 0$ otherwise. Assume that each video session can select at most one relay and each relay can at most be selected by one video session. We have,

$$\alpha_{s,r} \in \{0, 1\}, \forall s \in \mathcal{S}, \forall r \in \mathcal{R}, \quad (1)$$

$$\sum_{r \in \mathcal{R}} \alpha_{s,r} \leq 1, \forall s \in \mathcal{S}, \quad (2)$$

$$\sum_{s \in \mathcal{S}} \alpha_{s,r} \leq 1, \forall r \in \mathcal{R}. \quad (3)$$

Denote the maximum transmission power of each source and relay node as P_{\max}^s and P_{\max}^r , respectively. Then, it must hold

$$P_s \leq P_{\max}^s, \forall s \in \mathcal{S}, \quad (4)$$

$$P_r \leq P_{\max}^r, \forall r \in \mathcal{R}, \quad (5)$$

where P_s and P_r denote the transmission power of source s and relay r , respectively.

Assume that multiple concurrent transmissions are allowed on the same portion of the spectrum, e.g., through code division multiple access (CDMA) [19] or time-hopping impulse-radio ultra wide band (TH-IR-UWB) [20]. Denote the total available bandwidth as B , and the spreading gain as χ . We only consider long-term channel state information (CSI) and assume that the additive white Gaussian noise (AWGN) power perceived at each relay and destination node is equal to σ^2 .

The link capacity C_s for session s , can be expressed as

$$C_s = \left(1 - \sum_{r \in \mathcal{R}} \alpha_{s,r} \right) C_{s2d}^s + \sum_{r \in \mathcal{R}} \alpha_{s,r} C_{coop}^s, \quad (6)$$

where C_{s2d}^s and C_{coop}^s represent the direct link capacity and cooperative link capacity for session s , respectively.

1) *Direct link capacity C_{s2d}^s :* In the case where session s uses only a direct link, i.e., $\sum_{r \in \mathcal{R}} \alpha_{s,r} = 0$, we have

$$C_{s2d}^s = B \log_2 \left(1 + \frac{\chi G_{s2d}^{s,s} P_s}{\sigma^2 + I_{dst}^s} \right) \quad (7)$$

where $G_{s2d}^{s,s}$ represents the average channel gain from the source node of session s to the corresponding destination node, and I_{dst}^s is the average interference perceived at the destination node, which can in turn be expressed as

$$I_{dst}^s = \sum_{w \in \mathcal{S}, w \neq s} I_{dst,w}^{src,w} + \sum_{r \in \mathcal{R}} I_{dst,r}^{rly,r}. \quad (8)$$

In (8), $I_{dst,s}^{src,w}$ denotes the interference at the destination of session s caused by the source of session w , and $I_{dst,s}^{rly,r}$ denotes the interference at the destination of session s caused by relay node r .

Interference on each link depends on power allocation and relay selection at each individual node, but also on the network scheduling strategy at the media access control (MAC) layer (i.e., the relative synchronization of transmission start times between different network communication links). To keep the model treatable, the interference at each receiver can be approximated in different ways, e.g., worst-case approximation assuming that all source and active relay nodes cause interference in both time-slots, or average-based approximation which considers the average effect of each interferer over the two time slots. Our investigation reveals that the average-based approximation approximates reality very well - in-depth validation of the average-based interference model is discussed in detail in Appendix A. Then, if a video session, say w , uses a cooperative link, i.e., $\sum_{r \in \mathcal{R}} \alpha_{w,r} = 1$, the interference caused by the source of session w to the destination of session s can be expressed as

$$I_{dst,s}^{src,w} = \underbrace{\left(1 - \sum_{r \in \mathcal{R}} \alpha_{w,r}\right)}_{\text{direct link}} G_{s2d}^{w,s} P_w + \underbrace{\frac{1}{2} \left(\sum_{r \in \mathcal{R}} \alpha_{w,r}\right)}_{\text{cooperative link}} G_{s2d}^{w,s} P_w. \quad (9)$$

The other component in (8), $I_{dst,s}^{rly,r}$, represents the interference generated by relay node r at the destination of session s when it is used by another video session, i.e.,

$$I_{dst,s}^{rly,r} = \frac{1}{2} \sum_{w \in \mathcal{S}, w \neq s} \alpha_{w,r} G_{r2d}^{r,s} P_r, \quad (10)$$

where $G_{r2d}^{r,s}$ is the average channel gain from relay r to the destination of session s .

2) *Cooperative link capacity C_{coop}^s* : Assume that the decode-and-forward (DF) cooperative relaying mode is employed at each relay node. If session s uses the cooperative link, i.e., $\sum_{r \in \mathcal{R}} \alpha_{s,r} = 1$, we have

$$C_{coop}^s = \frac{1}{2} \min(C_{s2r}^s, C_{sr2d}^s), \quad (11)$$

where C_{s2r}^s is the capacity from source s to the selected relay node, and C_{sr2d}^s is the capacity achieved through maximal ratio combining of the received signals at the destination [2].

The link capacity from source node to relay node is modeled as

$$C_{s2r}^s = B \log_2 \left(1 + \frac{\chi \sum_{r \in \mathcal{R}} \alpha_{s,r} G_{s2r}^{s,r} P_s}{\sigma^2 + \sum_{r \in \mathcal{R}} \alpha_{s,r} I_{rly}^{r,s}} \right), \quad (12)$$

where $G_{s2r}^{s,r}$ is the average channel gain from the destination of session s to relay r , $I_{rly}^{r,s}$ is the interference perceived at relay r assuming that it is selected by session s , and consists of two components as $I_{rly}^{r,s} = I_{rly}^{r,s,src} + I_{rly}^{r,s,rly}$, where $I_{rly}^{r,s,src}$ represents the component of $I_{rly}^{r,s}$ caused by all other source

nodes, and $I_{rly}^{r,s,rly}$ represents the component of $I_{rly}^{r,s}$ caused by relay nodes. The two components can be expressed as

$$\begin{aligned} I_{rly}^{r,s,src} &= \underbrace{\sum_{w \in \mathcal{S}, w \neq s} \left(1 - \sum_{r \in \mathcal{R}} \alpha_{wr}\right) G_{s2r}^{w,r} P_w}_{\text{direct link}} \\ &\quad + \underbrace{\frac{1}{2} \sum_{w \in \mathcal{S}, w \neq s} \left(\sum_{r \in \mathcal{R}} \alpha_{wr}\right) G_{s2r}^{w,r} P_w,}_{\text{cooperative link}} \end{aligned} \quad (13)$$

$$I_{rly}^{r,s,rly} = \frac{1}{2} \sum_{u \in \mathcal{R}, u \neq r} \left(\sum_{w \in \mathcal{S}, w \neq s} \alpha_{w,u}\right) G_{r2r}^{u,r} P_u, \quad (14)$$

where $G_{r2r}^{u,r}$ represents the average channel gain from relay u to relay r .

Finally, the link capacity achieved through maximal ratio combining of the received signals at the destination in (11) can be expressed as

$$C_{sr2d}^s = B \log_2 \left(1 + \frac{\chi \left(G_{s2d}^{s,s} P_s + \sum_{r \in \mathcal{R}} \alpha_{s,r} G_{r2d}^{r,s} P_r \right)}{\sigma^2 + I_{dst}^s} \right), \quad (15)$$

where I_{dst}^s is defined in (8).

3) *Video Distortion Model*: The video quality is measured in terms of PSNR, which is a monotonically decreasing function of the mean-square error (MSE) [21]

$$\text{PSNR}_s = 10 \log_{10} (D_{\max}/D_s). \quad (16)$$

In (16), PSNR_s represents the PSNR of video session s , D_s is the corresponding video distortion, and D_{\max} is a constant parameter representing the maximum possible distortion.

Video distortion is caused by the interplay of lossy video compression, denoted as D_{enc}^s , and distortion caused by video packet loss, denoted as D_{los}^s ,

$$D_s = D_{enc}^s + D_{los}^s. \quad (17)$$

D_{enc}^s is a function of video encoding rate R_s , modeled as [21]

$$D_{enc}^s(R_s) = D_0^s + \frac{\theta_s}{R_s - R_0^s}, \quad D_0^s > 0, R_s > R_0^s, \quad \forall s \in \mathcal{S} \quad (18)$$

where D_0^s , R_0^s and θ_s are video-specific parameters.

Packet loss is caused by transmission errors and violations of the play-out deadline caused by queuing delay. We denote the packet error rate for video session s as P_{err}^s . For the sake of simplicity, we employ a simple $M/M/1$ model as in [22] - our model can be easily extended to account for more sophisticated delay models, e.g., a Chernoff-bound based model [23]. The average queuing delay T_{dly}^s of video session s can then be expressed as [24]

$$T_{dly}^s = L_s / (C_s - R_s), \quad (19)$$

where L_s , R_s and C_s are the average packet length, video encoding rate and link capacity for session s , respectively.

The probability that the queuing delay of a packet from video session s exceeds the play-out deadline T_0^s is then $P_{dly}^s = e^{-(C_s - R_s)T_0^s/L_s}$.

The distortion caused by packet loss D_{los}^s in (17) can then be formulated as $D_{los}^s = k_s(P_{err}^s + (1 - P_{err}^s)P_{dly}^s)$, where k_s is a parameter representing the sensitivity of a video sequence to packet loss, which can be measured off-line or estimated in real time.

B. SUM PSNR Maximization Problem

The problem can be formulated as that of maximizing the sum PSNR of multiple video sessions, by jointly controlling the video encoding rate, power allocation and relay selection, subject to a set of constraints as follows.

- **Minimum rate:** Each video session requires a minimum encoding rate R_0^s for video session s , i.e.,

$$R_s \geq R_0^s, \forall s \in \mathcal{S}. \quad (20)$$

- **Link capacity:** The video encoding rate for each video session cannot exceed the available link capacity, i.e., $R_s \leq C_s, \forall s \in \mathcal{S}$.
- **Queuing delay:** The average queuing delay for each video session cannot exceed the play-out deadline, i.e., $T_{dly}^s \leq T_0^s, \forall s \in \mathcal{S}$. By substituting (19) into the constraint, we have

$$R_s \leq C_s - L_s/T_0^s. \quad (21)$$

Therefore, the link capacity constraint is implied by the queuing delay constraint.

- **Maximum transmission power:** The transmission power of each source and relay node is limited by the maximum transmission power as in (4) and (5).
- **Relay selection:** Relay assignment has to satisfy constraints expressed as in (1), (2) and (3).

Define $\mathbf{P} = \{P_s, P_r | \forall s \in \mathcal{S}, r \in \mathcal{R}\}$, $\mathbf{R} = \{R_s | \forall s \in \mathcal{S}\}$, and $\boldsymbol{\alpha} = \{\alpha_{s,r} | s \in \mathcal{S}, r \in \mathcal{R}\}$ as the vectors of power allocation strategy, video encoding rate, and relay selection strategy, respectively. Then, the problem can be formulated as

$$\begin{aligned} Given : & G_{s2d}^{w,s}, G_{r2d}^{r,s}, G_{r2r}^{u,r}, R_0^s, D_0^s, \theta_s, \\ & P_{\max}^s, P_{\max}^r, w, s \in \mathcal{S}, u, r \in \mathcal{R} \end{aligned} \quad (22)$$

$$Find : \boldsymbol{\alpha}, \mathbf{P}, \mathbf{R} \quad (23)$$

$$Maximize : \sum_{s \in \mathcal{S}} \text{PSNR}_s \quad (24)$$

$$Subject to : (1), (2), (3), (4), (5), (20), (21) \quad (25)$$

It is worth pointing out that, although the problem formulation in this section focuses on video streaming only, it can be extended to account for heterogeneous traffic sources.

III. DISTRIBUTED SOLUTION ALGORITHM

In this section, we propose a distributed solution algorithm for the problem formulated in Section II. Then, in Section V, we evaluate the distributed algorithm by comparing it to a centralized algorithm proposed in Section IV.

For reasons that will become clearer after comparison with the globally optimal algorithm, we do not consider power control in the distributed algorithm, and each source and relay node is allowed to transmit at its maximum power. As shown in Section V an almost-optimal network performance can be achieved by the distributed algorithm without power control compared to the globally optimal algorithm developed in Section IV.

With fixed maximum transmission power, the problem of video rate control and relay selection can be formulated as a series of coupled optimization problems in which each video session is an agent. Each agent optimizes its own video quality by selecting (selfishly) optimal relay node and video encoding rate. Denote the vector of relay selection strategies for video session $s \in \mathcal{S}$ as $\boldsymbol{\alpha}_s = (\alpha_{s,r})$, $r \in \mathcal{R}$, and the vector of relay selection strategy for all video sessions except s as $\boldsymbol{\alpha}_{-s} = (\alpha_{w,r})$, $r \in \mathcal{R}$, $w \in \mathcal{S}$, $w \neq s$. Further define the vector of video encoding rates of all sessions except s as $\mathbf{R}_{-s} = (R_w)$, $w \in \mathcal{S}$, $w \neq s$. Then, the objective of each agent is to find a solution to

$$(\boldsymbol{\alpha}_s^*, R_s^*) = \arg \max_{\boldsymbol{\alpha}_s, R_s} \text{PSNR}_s(\boldsymbol{\alpha}_s, R_s, \boldsymbol{\alpha}_{-s}^*, \mathbf{R}_{-s}^*) \quad (26)$$

$$Subject to : (1), (2), (3), (20), (21).$$

To this end, we propose an algorithm in which each player locally optimizes its own video quality by solving the optimization problem in (26) as follows.

Recall that PSNR_s is a concave function of video encoding rate and link capacity. With given fixed transmission power of all source and relay nodes, and also relay selection strategy for all other video sessions except s , the overall link capacity for video session s in (6) can be reformulated as a linear function of relay selection variable $\alpha_{s,r}$, $r \in \mathcal{R}$

$$C_s = \left(1 - \sum_{r \in \mathcal{R}} \alpha_{s,r} \right) C_{s2d}^s + \sum_{r \in \mathcal{R}} \alpha_{s,r} C_{coop}^{s,r}, \quad (27)$$

where C_{s2d}^s and $C_{coop}^{s,r}$ are constants that represent the capacity of direct link and cooperative link if relay node r is used by video session s , respectively. Since this composition preserves convexity [25], the objective function of PSNR_s is also a concave function of $\alpha_{s,r}$, $r \in \mathcal{R}$.

Considering that PSNR_s is also a monotonically increasing function of the link capacity, maximizing PSNR_s can be decomposed into two subproblems: i) maximizing link capacity by solving a linear optimization problem with objective function defined in (27), and ii) maximizing PSNR_s by solving a convex optimization as follows

$$Given : C_s \quad (28)$$

$$Find : R_s \quad (29)$$

$$Maximize : \text{PSNR}_s \quad (30)$$

$$Subject to : (20), (21). \quad (31)$$

Without loss of generality, we assume that in the first subproblem, $C_{s2d}^s \neq C_{coop}^{s,r}$, $r \in \mathcal{R}$ and $C_{coop}^{s,r} \neq C_{coop}^{s,q}$, $r, q \in$

\mathcal{R} , $r \neq q$. Then, constraint in (1) is equivalent to

$$0 \leq \alpha_{s,r} \leq 1, \quad s \in \mathcal{S}, \quad r \in \mathcal{R}. \quad (32)$$

Hence, constraints in (1), (2), (3), (20), (21) form a convex domain set, and the problem formulated in (26) is a convex optimization problem that can be solved efficiently using interior-point methods [17].

IV. GLOBALLY OPTIMAL ALGORITHM

The problem formulated in Section II-B is a nonlinear, non-convex combinatorial problem. In general, MINLP problems are NP-HARD, i.e., no existing algorithm can solve an arbitrary MINLP in polynomial time. In order to provide a performance benchmark for evaluation of the proposed distributed algorithm, we propose a solution algorithm based on the *branch-and-bound* framework and on convex relaxation techniques. The algorithm is designed to solve the problem with very low complexity in practice compared to an exhaustive search. To the best of our knowledge, this is the first algorithm that addresses optimal video rate control, relay selection and power control in interference-limited wireless networks.

A. Basic Steps of the Proposed Algorithm

The proposed algorithm searches for a globally optimal solution with predefined precision of optimality $0 < \epsilon \leq 1$. Denote f^* as the globally optimal sum PSNR objective function as, then the algorithm searches for a ϵ -optimal solution f , which satisfies $f \geq \epsilon f^*$.

We let $\mathcal{Q}_0 = \{\mathbf{P}, \mathbf{R}, \boldsymbol{\alpha}\}$ represent the original search space (including all possible combinations of video rate control, power allocation and relay selection). The proposed algorithm partitions \mathcal{Q}_0 iteratively into a set of sub-domains $\mathbf{Q} = \{\mathcal{Q}_i \subset \mathcal{Q}_0, i = 1, 2, \dots\}$, where i represents the iteration step of the algorithm.

For each \mathcal{Q}_i , the algorithm calculates a local upper bound $UP(\mathcal{Q}_i)$ and a local lower bound $LR(\mathcal{Q}_i)$, on the objective function of sum PSNR. To calculate a local upper bound, we relax the original non-convex combinatorial problem into two convex problems. Then, based on the solution of the relaxed problems, we locally search for a feasible solution and set the corresponding sum PSNR as a local lower bound.

The proposed algorithm also maintains a global upper bound UP_{glb} and global lower bound LR_{glb} on the sum PSNR. At each iteration of the algorithm, the two global bounds are updated as follows

$$UP_{\text{glb}} = \max\{UP(\mathcal{Q}_i), i = 1, 2, \dots\}, \quad (33)$$

$$LR_{\text{glb}} = \max\{LR(\mathcal{Q}_i), i = 1, 2, \dots\}. \quad (34)$$

Then, if $LR_{\text{glb}} \geq \epsilon \cdot UP_{\text{glb}}$, the algorithm terminates and sets the optimal sum PSNR to $f^* = LR_{\text{glb}}$. Otherwise, the algorithm chooses one sub-domain from \mathbf{Q} and further partitions it into two sub-domains. In our algorithm, we select the \mathcal{Q}_i with the highest local upper bound, i.e., $i = \arg \max_i UP(\mathcal{Q}_i)$.

If $UP(\mathcal{Q}_i) < LR_{\text{glb}}$, this indicates that the globally optimal solution f^* is not located in \mathcal{Q}_i , then, \mathcal{Q}_i is removed from \mathbf{Q} .

The algorithm could be guaranteed to converge to the globally optimal sum PSNR f^* . An intuitive proof of the convergence is given in Appendix B.

B. Convex-Relaxation

In this section, we derive a relaxation of the original problem by applying reformulation linearization techniques [26]. Through the proposed relaxation, at each iteration of the algorithm, the problem can be solved in polynomial time on a restricted domain using standard convex optimization techniques to provide an upper bound on the sum PSNR.

First, we need to state the following lemma:

Lemma 1: The objective function in (24) is a concave function of video encoding rate \mathbf{R} and link capacity \mathbf{C} .

Proof of Lemma 1 is based on the fact that *a function is concave if and only if it is concave when restricted to any line in its domain* [25]. Due to limited space, detailed proof is omitted. Based on: (i) Lemma 1, (ii) the fact that PSNR is nondecreasing with respect to C_s , (iii) the composition property that preserves convexity [25], to relax the original problem to a convex problem we only need to relax C_s such that it is a concave function of P_s , P_r and $\alpha_{s,r}$, and hence the queuing delay constraint in (21) becomes convex.

From the link capacity model in Section II-A, we can see that the expression of the overall link capacity, defined in (6)–(15), is rather involved. To simplify the convex relaxation, we designed a two-stage relaxation method, whose key idea can be intuitively illustrated as follows:

- For a given sub-domain \mathcal{Q}_i , if the relay selection strategy $\alpha_{s,r}$ in \mathcal{Q}_i is not fixed for all s and r , we only relax $\alpha_{s,r}$ but assume that the network is interference-free. Denote the relaxation in this stage as **RLX_1**.
- Given a sub-domain \mathcal{Q}_i , if the relay selection strategy $\alpha_{s,r}$ in \mathcal{Q}_i is fixed for all s and r , we relax P_s and P_r . Denote the relaxation in this stage as **RLX_2**.

Next, **RLX_1** is taken as an example to show how to relax the original problem formulated in Section II to be convex, while relaxation for **RLX_2** can be performed similarly.

RLX_1: Based on the assumption of interference-free network, each node can work at its maximum transmission power, and the link capacity is a function of $\alpha_{s,r}$ only. Then, the link capacity from source to destination C_{s2d}^s defined in (7) can be relaxed as

$$C_{s2d}^s = B \log_2 \left(1 + \chi G_{s2d}^{s,s} P_{\max}^s / \sigma^2 \right), \quad (35)$$

while capacities C_{s2r}^s in (12) and C_{sr2d}^s in (15) can be relaxed similarly to C_{s2d}^s .

The cooperative link capacity, C_{coop}^s defined in (11), can be expressed with two constraints as

$$\begin{cases} C_{\text{coop}}^s \leq \frac{1}{2} C_{s2r}^s \\ C_{\text{coop}}^s \leq \frac{1}{2} C_{sr2d}^s \end{cases}. \quad (36)$$

Notice that the C_{coop}^s is nondecreasing with C_{s2r}^s and C_{sr2d}^s .

We also need to relax the overall link capacity C_s defined in (6). We first relax the relay selection strategy by allowing each relay to be assigned to multiple video sessions, and vice

versa, allowing each video session to use multiple relays. Then the constraint in (1) can be rewritten as

$$\alpha_{\min}^{s,r} \leq \alpha_{s,r} \leq \alpha_{\max}^{s,r}, \forall s \in \mathcal{S}, r \in \mathcal{R}, \quad (37)$$

where $\alpha_{\min}^{s,r}$ and $\alpha_{\max}^{s,r}$ are the lower and upper bounds on $\alpha_{s,r}$, respectively. At the first iteration, they are set to $\alpha_{\min}^{s,r} = 0$, and $\alpha_{\max}^{s,r} = 1$, $\forall s \in \mathcal{S}, r \in \mathcal{R}$. Denote $C_{\max}^{coop,s}, C_{\min}^{coop,s}$ as an upper and lower bound for C_{coop}^s , respectively, and further denote the nonlinear item in (6), $\alpha_{s,r} C_{\text{coop}}^s$ with $\beta_{\text{coop}}^{s,r}$. Then, according to the *reformulation and linearization technique* (RLT), $\beta_{\text{coop}}^{s,r}$ can be relaxed using four linear constraints as

$$\begin{cases} (\alpha_{\max}^{s,r} - \alpha_{s,r})(C_{\max}^{coop,s} - C_{\text{coop}}^s) \geq 0 \\ (\alpha_{\max}^{s,r} - \alpha_{s,r})(C_{\text{coop}}^s - C_{\min}^{coop,s}) \geq 0 \\ (\alpha_{s,r} - \alpha_{\min}^{s,r})(C_{\max}^{coop,s} - C_{\text{coop}}^s) \geq 0 \\ (\alpha_{s,r} - \alpha_{\min}^{s,r})(C_{\text{coop}}^s - C_{\min}^{coop,s}) \geq 0 \end{cases} \quad (38)$$

and then substituting $\alpha_{s,r} C_{\text{coop}}^s$ into (38).

The lower bound for C_{coop}^s can be simply set to be $C_{\min}^{coop,s} = 0$. An upper bound can be obtained as,

$$C_{\max}^{coop,s} = \max(C_{\max}^{s2r,s}, C_{\max}^{sr2d,s})/2, \quad (39)$$

where $C_{\max}^{s2r,s} = B \log_2 (1 + \chi P_{\max}^{\text{tmp},s} / \sigma^2)$ and $C_{\max}^{sr2d,s} = B \log_2 (1 + \chi (G_{s2r}^{s,r} P_{\max}^s + P_{\max}^{\text{tmp},r}) / \sigma^2)$, with $P_{\max}^{\text{tmp},s} = \max(G_{s2r}^{s,r} P_{\max}^s \alpha_{\max}^{s,r})$ and $P_{\max}^{\text{tmp},r} = \max_{r \in \mathcal{R}} (G_{r2d}^{r,s} P_{\max}^r \alpha_{\max}^{s,r})$ for any $\forall s \in \mathcal{S}$.

Notice that, when calculating the upper bound, the relaxation to $\alpha_{s,r}$ in (37) is not taken into consideration. The overall link capacity C_s in (6) can then be expressed as

$$C_s = \left(1 - \sum_{r \in \mathcal{R}} \alpha_{s,r}\right) C_{s2d}^s + \sum_{r \in \mathcal{R}} \beta_{\text{coop}}^{s,r}. \quad (40)$$

So far, we have relaxed the original problem such that i) C_s in (40) is linear function of $\alpha_{s,r}$, C_{s2d}^s and $\beta_{\text{coop}}^{s,r}$, ii) C_{s2d}^s in (35) is a constant, iii) $\beta_{\text{coop}}^{s,r}$ defined in (38) is constrained by $\alpha_{s,r}$ and C_{coop}^s through four linear functions, and iv) constraints in (36) result in a convex domains. Together with Lemma (1), the relaxed problem is a convex optimization problem in standard form.

C. Local Search Method

In each iteration of our algorithm, we solve the RLX_1 or RLX_2 using interior-point algorithms [17]. However, the optimal relaxed solution may not be feasible. For example, in the case of RLX_1, the optimal $\alpha_{s,r}^*$ is likely to take an intermediate value between 0 and 1. We call this optimal solution the relaxed solution. Then, we locally search for a feasible solution starting from the relaxed solution, and set the corresponding sum PSNR as a lower bound to the original problem. The local search is based on the fact that the power allocation in the relaxed solution is always feasible. A feasible value of $\alpha_{s,r}$ can be set to its closest integer, i.e., $\alpha_{s,r} = \text{round}(\alpha_{s,r}^*)$. Note that because of the constraints in (2) and (3), there exists at most one r over all $s \in \mathcal{S}$, and one s over all $r \in \mathcal{R}$, such that $\text{round}(\alpha_{s,r}^*) = 1$.

Given a feasible power allocation and relay selection, a feasible $C_{s2d}^s, C_{\text{coop}}^s$ and further C_s , can be calculated using (7), (15) and (6), respectively. Given C_s , the optimal video encoding rate R_s for session s and the optimal sum PSNR can be calculated by solving the following convex problem

$$\text{Given : } C_s, s \in \mathcal{S} \quad (41)$$

$$\text{Find : } R_s, s \in \mathcal{S} \quad (42)$$

$$\text{Maximize } \sum_{s \in \mathcal{S}} \text{PSNR}_s \quad (43)$$

$$\text{Subject to : } (20), (21). \quad (44)$$

D. Domain Partition

We first need to select a sub-domain from \mathcal{Q} to be partitioned. Considering that the global upper bound is equal to the highest local lower bound, we select the \mathcal{Q}_i with the highest local upper bound to be partitioned, such that the global upper bound becomes smaller as partition progresses. To partition \mathcal{Q}_i into two sub-domains, we need to select a variable among $\alpha_{s,r}$, P_s and P_r , and then partition it from a middle value of its domain. Here, only variables that affect the sum PSNR directly are partitioned, i.e., no intermediate variables are partitioned, e.g., $\beta_{\text{coop}}^{s,r}$ in (11).

At the beginning of the algorithm, there is only one domain \mathcal{Q}_0 in \mathcal{Q} , and the relay selection is not fixed. In this case, the RLX_1 is employed to calculate the local upper bound. Denote $\alpha_{s,r}^*$ as the relaxed solution to $\alpha_{s,r}$. Then α_{s^*,r^*}^* is selected for partition over all $s \in \mathcal{S}$ and $r \in \mathcal{R}$ such that

$$\alpha_{s^*,r^*}^* = \max_{s \in \mathcal{S}, r \in \mathcal{R}} \{(\alpha_{\max}^{s,r} - \alpha_{\min}^{s,r}) \cdot \alpha_{s,r}^*\}. \quad (45)$$

Since a higher value of $\alpha_{s,r}$ indicates that relay r is more likely to be assigned to video session s , the above criterion fixes the relay assignment decision with the highest value of $\alpha_{s,r}$. Note that as the variable partition goes, the value $\alpha_{s,r}$ would be fixed for some s and r . The item $(\alpha_{\max}^{s,r} - \alpha_{\min}^{s,r})$ in (45) is introduced to avoid selecting $\alpha_{s,r}$ with $\alpha_{\max}^{s,r} = \alpha_{\min}^{s,r} = 1$. Then, the selected α_{s^*,r^*}^* is partitioned by setting $\alpha_{\max}^{s^*,r} = 0, \forall r \in \mathcal{R}, r \neq r^*, \alpha_{\max}^{s,r^*} = 0, \forall s \in \mathcal{S}, s \neq s^*$, and $\alpha_{\min}^{s^*,r^*} = 1$ for the first new sub-domain and $\alpha_{\max}^{s^*,r^*} = 0$ for the second new sub-domain.

After a certain number of variable partitions, in the selected \mathcal{Q}_i the relay selection strategy could be fixed. Denote

$$\Delta P_{s^*} = \max_{s \in \mathcal{S}} \{P_{\max}^s - P_{\min}^s\}, \quad (46)$$

$$\Delta P_{r^*} = \max_{r \in \mathcal{R}} \left\{ (P_{\max}^r - P_{\min}^r) \cdot \max_{s \in \mathcal{S}} (\alpha_{\max}^{s,r}) \right\}. \quad (47)$$

Then, if $\Delta P_{s^*} \geq \Delta P_{r^*}$, P_{s^*} is partitioned by setting $P_{\max}^{s^*|new} = P_{\min}^{s^*} + \Delta P_{s^*}/2$ for the first new sub-domain, and $P_{\min}^{s^*|new} = P_{\min}^{s^*} + \Delta P_{s^*}/2$ for the second new sub-domain. Otherwise, the P_{r^*} is partitioned similarly. Here, $P_{\max}^{s^*|new}$ and $P_{\min}^{s^*|new}$ mean the upper and lower bounds for P_s in the new sub-domains, respectively. In (47), the item $\max_{s \in \mathcal{S}} (\alpha_{\max}^{s,r})$ is introduced to avoid partitioning the power of relay node, say r , with $\alpha_{\max}^{s,r} = 0$ for all $s \in \mathcal{S}$.

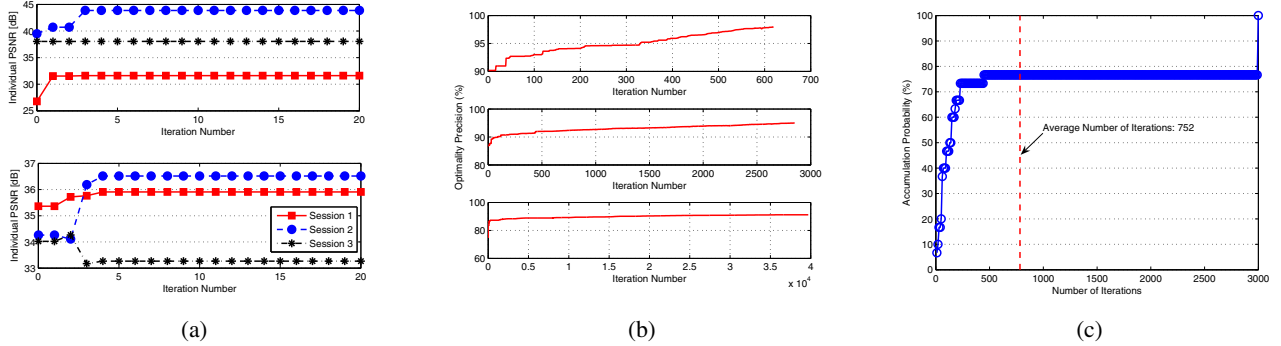


Fig. 1: (a) Convergence performance of the distributed algorithm. (b) Convergence performance of the centralized algorithm. (c) Complexity performance of the centralized algorithm, measured in accumulation probability of required number of iterations to converge.

TABLE I: Video Parameters

Video	D_0	θ	R_0	P_r	k	T	L
FM	0.38	2537	18.3	0.01	750	350	3040
MD	0	857	0.67	0	30	350	3040

V. SIMULATION RESULTS

In this section, performance evaluation results are presented for the proposed distributed and centralized algorithms. We consider a communication area of 1000×600 m². Different network scales are considered including N nodes, with $N = 10, 20, 30, 50$ and 100 . Nodes are randomly distributed in the communication area. The path loss coefficient between node s and node d is given by $G_{s,d}^2 = \|s-d\|^{-4}$, where $\|s-d\|$ represents the distance [m] between the two nodes, and 4 is the path loss factor. AWGN noise power is set to 10^{-7} mW for each node. The bandwidth of the available spectrum is set to $B = 200$ kHz and the spreading gain is set to $\chi = 10$. The maximum transmission power for each source and relay node is set to 1000 mW. Two video sequences are considered, *Foreman* (FM) and *Mother and Daughter* (MD), which are characterized by intense and moderate movement of the video. The parameters of the two video sequences are reported in Table I, where the unit for R_0 , T , and L are Kbits/s, ms and bits, respectively. We first show convergence and complexity analysis for the proposed distributed and centralized algorithms. Then, we provide performance comparison results between the two algorithms. These are obtained by averaging over 30 simulations.

Convergence performance of the proposed distributed algorithm is shown in Fig. 1 (a) in terms of individual PSNR with three video sessions, FM, MD and FM and in cases of total number of nodes of 20 for the top figure and 50 for the bottom figure. We can see that in both cases, the distributed can converges very fast in less than five iterations.

Convergence performance of the proposed optimal algorithm is shown in Fig. 1 (b) in cases of different video sessions, total number of nodes, and also maximum optimality precision. Network parameters are set to (FM, MD, 30, 98%) for the top figure, (FM, MD, FM, 30, 95%) for the middle

figure, and (FM, MD, 100, 90%) for the bottom figure, respectively. In the figures, optimality precision is defined as the ratio of global lower bound on sum PSNR to the global upper bound. We can see that in all three cases, the centralized algorithm converges to the predefined optimality precision.

The complexity of the optimal algorithm is evaluated in terms of average number of iterations, and accumulation probability of required number of iterations are shown in Fig. 1 (c) in the case of (FM, MD, 30, 95%). Results are obtained by averaging over 30 times of independent simulations. We can see that the number of iterations varies from 7 to 3000 with an average of 752. We observe that, around 80% of simulations can be finished in less 500 iterations. Recall that our algorithm searches for the ϵ -optimal solution by partitioning the original domain into a series of sub-domains. In this simulation, there are two video sessions and 30 nodes in total. Hence, there are 2 source nodes and 26 potential relay nodes, and then, number of relay selection variables $\alpha_{s,r}$, $s \in \mathcal{S}$, $r \in \mathcal{R}$, is $2 \times 26 = 52$. We quantize the maximum transmission power of 1000 mW using a step of 100 mW, then, each source or relay node has 10 possible choices of transmission power. Then, total number of possible transmission strategies can be calculated as $2^{52} \times (2+26)^{10} \approx 1.3 \times 10^{30}$, which is too large to search the original domain exhaustively. Therefore, compared to the an exhaustive search, the proposed centralized algorithm is quite efficient in computational complexity.

Performance for the proposed distributed and centralized algorithms are shown in Fig. 2 in terms of sum PSNR. Results are obtained by averaging over 30 times of independent simulations. In the figure, the algorithm with fixed maximum transmission power and without cooperation is employed as bottom-line performance. Two video sessions of FM and MD are employed and the total number of nodes is set to 20 and 30, respectively. We can see that the proposed centralized algorithm can achieve the highest sum PSNR. In the case of 30 nodes, an improvement greater than 2 dB can be achieved compared to the algorithm with fixed power and without cooperation. Sum PSNR achieved by the proposed distributed algorithm is very close to the centralized algorithm in the case of 20 nodes. Compared to the algorithm with fixed power

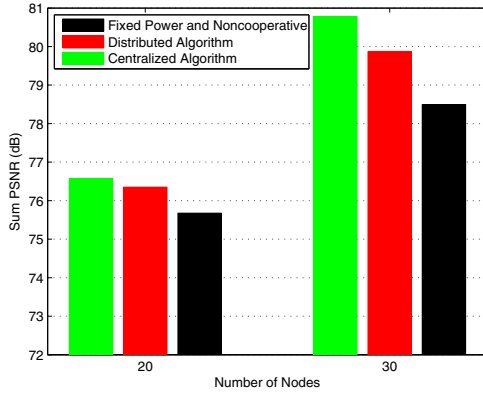


Fig. 2: Performance in sum PSNR for the proposed centralized and distributed algorithms.

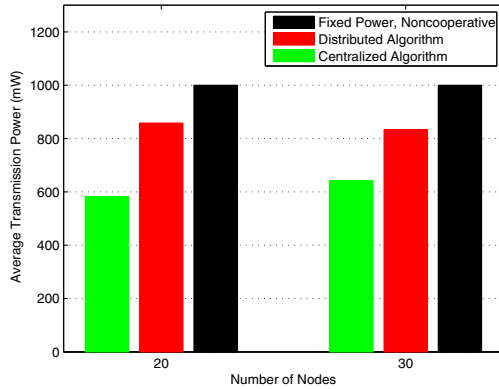


Fig. 3: Performance in average transmission power for the proposed distributed and centralized algorithms.

and without cooperation, the distributed algorithm can achieve about 1.5 dB of improvement by using cooperative relaying in the case of 30 nodes.

The proposed two algorithms are also evaluated in terms of average transmission power, which is averaged over two time-slots, all source nodes and the selected relay nodes. Results are shown in Fig. 3. With the proposed centralized algorithm, nodes are allowed to transmit at low power level. In the experiments, irrespective of whether a cooperative relay is used or not, each source and relay node if selected always transmits at a power that is close to the maximum. By using cooperative relays, the transmission time for each source and relay is half compared to the case of direct transmission. Consequently, the total transmission power becomes more evenly distributed over the whole network. This is extremely important in wireless multimedia sensor networks to avoid depleting a single node and hence to avoid bottleneck links. Our distributed algorithm is designed based on this observation. Even if the maximum transmission power is used for each source and relay node, the distributed algorithm can achieve more even power consumption through cooperative relaying.

VI. CONCLUSIONS

In this paper, we have studied cross-layer design techniques for cooperative video streaming in wireless networks. We formulated the problem of joint control of the video encoding rate, relay selection and power allocation as a non-convex and combinatorial problem. Then, we proposed a distributed algorithm, which is suboptimal but simple and easy to implement. We showed that the distributed algorithm can converge very quickly to a solution very closed to the global optimum. We also proposed a globally optimal solution algorithm based on a combination of branch and bound and convex relaxation of the original problem. Through numerical results, we showed that the algorithm can always converge to the optimal solution. Moreover, we have shown that through cooperative relaying nodes are allowed to work at lower level of average transmission power without decrease in the sum video quality. Moreover, compared to globally optimal solution the distributed algorithm was proven to achieve a good video performance. The proposed algorithm can be directly applied to a scenario with multiple co-existing pre-established source-destination pairs, and can be also used to optimally control resource allocation for an independent set of transmissions with primary interference constraints (i.e., no transmitters and receivers in common) periodically scheduled by a separate scheduling algorithm, where idle nodes can be used as potential relays.

REFERENCES

- [1] V. Tarokh, N. Seshadri, and A. R. Calderbank, "Space-time Codes for High Data Rate Wireless Communication: Performance Criterion and Code Construction," *IEEE Trans. on Information Theory*, vol. 44, no. 2, pp. 744–765, March 1998.
- [2] J. N. Laneman, D. N. C. Tse, and G. W. Wornell, "Cooperative Diversity in Wireless Networks: Efficient Protocols and Outage Behavior," *IEEE Trans. on Information Theory*, vol. 50, no. 12, pp. 3062–3080, Dec. 2004.
- [3] G. Jakllari, S. V. Krishnamurthy, M. Faloutsos, P. V. Krishnamurthy, and O. Ercetin, "A Cross-Layer Framework for Exploiting Virtual MISO Links in Mobile Ad Hoc Networks," *IEEE Trans. on Mobile Computing*, vol. 6, no. 6, pp. 579–594, Jun. 2007.
- [4] G. Kramer, I. Maric, and R. D. Yates, "Cooperative Communications," *Foundations and Trends in Networking*, vol. 1, no. 3-4, pp. 271–425, Jun. 2007.
- [5] K. J. R. Liu, K. Ahmed, W. Su, and K. Andres, *Cooperative Communications and Networking*. Cambridge, U.K.: Cambridge University Press, 2009.
- [6] A. H.-Madsen and J. Zhang, "Capacity Bounds and Power Allocation for Wireless Relay Channels," *IEEE Trans. on Information Theory*, vol. 51, no. 6, pp. 2020–2040, Jun. 2005.
- [7] G. Kramer, M. Gastpar, and P. Gupta, "Cooperative Strategies and Capacity Theorems for Relay Networks," *IEEE Trans. on Information Theory*, vol. 51, no. 9, pp. 3037–3063, Sept. 2005.
- [8] P. Liu, Z. Tao, S. Narayanan, T. Korakis, and S. S. Panwar, "CoopMAC: A Cooperative MAC for Wireless LANs," *IEEE Journal on Selected Areas in Commun. (JSAC)*, vol. 25, no. 2, pp. 340–354, Feb. 2007.
- [9] S. Lakshmanan and R. Sivakumar, "Diversity Routing for Multi-hop Wireless Networks with Cooperative Transmissions," in *Proc. of 6th Annual IEEE Communications Society Conference on Sensor, Mesh and Ad Hoc Communications and Networks (SECON)*, pp. 1–9, Rome, Italy, Jun. 2009.
- [10] J. Zhang and Q. Zhang, "Cooperative Routing in Multi-Source Multi-Destination Multi-hop Wireless Networks," in *Proc. of the 27th IEEE International Conference on Computer Communications (INFOCOM)*, pp. 2369–2377, Phoenix, AZ, Apr. 2008.

- [11] Y. Shi, S. Sharma, Y. T. Hou, and S. Kompella, "Optimal relay assignment for cooperative communications," in *Proc. ACM Intern. Symp. on Mobile Ad Hoc Networking and Computing (MobiHoc)*, pp. 3–12, Hong Kong SAR, China, May 2008.
- [12] S. Sharma, Y. Shi, Y. T. Hou, H. D. Sherali, and S. Kompella, "Cooperative Communications in Multi-hop Wireless Networks: Joint Flow Routing and Relay Node Assignment," in *Proc. of 29th IEEE International Conference on Computer Communications (INFOCOM)*, pp. 1–9, San Diego, CA, USA, Mar. 2010.
- [13] E. M. Yeh and R. A. Berry, "Throughput Optimal Control of Cooperative Relay Networks," *IEEE Trans. on Information Theory*, vol. 53, no. 10, pp. 3827–3833, Oct. 2007.
- [14] J. Jin and B. Li, "Cooperative Resource Management in Cognitive WiMAX with Femto Cells," in *Proc. of 29th IEEE International Conference on Computer Communications (INFOCOM)*, pp. 1–9, San Diego, CA, USA, Mar. 2010.
- [15] H. Xu and B. Li, "Efficient Resource Allocation with Flexible Channel Cooperation in OFDMA Cognitive Radio Networks," in *Proc. of 29th IEEE International Conference on Computer Communications (INFOCOM)*, pp. 1–9, San Diego, CA, USA, Mar. 2010.
- [16] S. Sharma, Y. Shi, J. Liu, Y. T. Hou, and S. Kompella, "Is Network Coding Always Good for Cooperative Communications?," in *Proc. of 29th IEEE International Conference on Computer Communications (INFOCOM)*, pp. 1–9, San Diego, CA, USA, Mar. 2010.
- [17] Y. E. Nesterov and A. S. Nemirovskii, *Interior Point Polynomial Algorithms in Convex Programming*. SIAM, Philadelphia, 2004.
- [18] S. Pudlewski and T. Melodia, "A Distortion-minimizing Rate Controller for Wireless Multimedia Sensor Networks," *Computer Communications (Elsevier)*, vol. 33, no. 12, pp. 1380–1390, July 2010.
- [19] A. J. Viterbi, *CDMA: Principles of Spread Spectrum Communication*. Addison-Wesley, 1995.
- [20] T. Melodia and I. F. Akyildiz, "Cross-layer QoS-Aware Communication for Ultra Wide Band Wireless Multimedia Sensor Networks," *IEEE Journal of Selected Areas in Communications*, vol. 28, pp. 653–663, June 2019.
- [21] K. Stuhlmüller, N. Fäber, M. Link, and B. Girod, "Analysis of Video Transmission Over Lossy Channels," *IEEE Journal on Selected Areas in Commun. (JSAC)*, vol. 18, no. 6, pp. 1012–1032, Jun. 2000.
- [22] X. Zhu, E. Setton, and B. Girod, "Congestion-Distortion Optimized Video Transmission Over Ad Hoc Networks," *EURASIP Signal Processing: Image Communication*, vol. 20, no. 8, pp. 773–783, Sept. 2005.
- [23] H. Chernoff, "A Measure of Asymptotic Efficiency for Tests of A Hypothesis Based on The Sum of Observations," *The Annals of Mathematical Statistics*, vol. 23, no. 4, pp. 493–507, Dec. 1952.
- [24] D. Bertsekas and R. Gallager, *Data Networks*. USA: Prentice Hall, 2000.
- [25] S. Boyd and L. Vandenberghe, *Convex Optimization*. Cambridge University Press, 2004.
- [26] H. D. Sherali and W. P. Adams, *A Reformulation-Linearization Technique for Solving Discrete and Continuous Nonconvex Problems*. Boston: MA: Kluwer Academic, 1999.

APPENDIX

A. Validation of The Average-Based Interference Model

We validate the average interference model by comparing it to the exact interference in practical cooperative wireless networks. Let us consider a cooperative network with global time-synchronization, in which all source nodes transmit in the first time-slot while all relay nodes transmit in the second. Then, for a wireless link l that uses direct transmission only, the interference measured at its destination node comes from all source nodes of a number N_{itf} of cooperative sessions in the first time-slot, while it comes from all relay nodes in the second. Then, the average capacity of the wireless link C_{rea} can be calculated as $C_{rea} = \frac{1}{2}(C_{slot1} + C_{slot2})$, where C_{slot1} and C_{slot2} represent the capacity in the first and second time-slot, respectively.

Use C_{avg} to represent capacity of the wireless link l calculated using the average-based interference model and then we compare it to C_{rea} . A communication area of $1000 \times 1000 \text{ m}^2$ is considered and the number of interfering cooperative sessions varies from 2 to 16 with a step of 2. Other simulation parameters are set as in Section II. Results of the comparison in terms of $\frac{C_{avg}}{C_{rea}}$ are shown in Fig. 4. Every point was plotted by averaging over 10^3 simulations. The value of C_{avg}

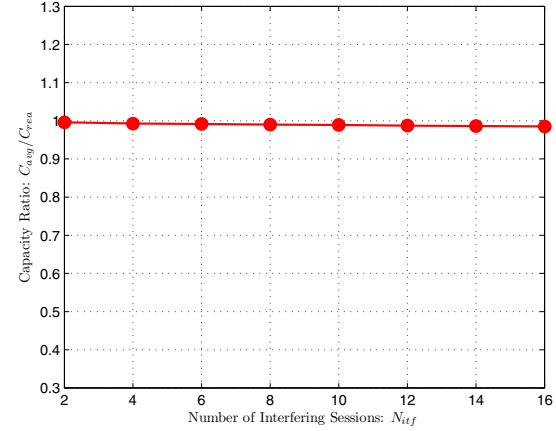


Fig. 4: Comparison between the average-based interference model and exact interference in synchronization-based cooperative network.

is slightly lower but very close to that of C_{rea} , e.g., more than 99% and 98% of C_{rea} can be achieved when $N_{itf} = 2$ and $N_{itf} = 16$, respectively. We observe that the value of $\frac{C_{avg}}{C_{rea}}$ decreases very slightly as the number of interfering sessions increases, implying that the accumulation of performance degradation caused by the average-based interference model is negligible. Similar results can be also observed when wireless link l also uses cooperative relaying. Based on the above discussion, we can conclude that *the average-based interference model performs very well in tracking the cumulative effect of interference from different sources in practical cooperative wireless networks*.

B. Proof of Convergence of The Proposed Globally Optimal Algorithm

As the domain-partition progresses, the algorithm converges to the globally optimal sum PSNR f^* . This can be guaranteed by the following two properties of our algorithm.

First, as $i \rightarrow \infty$, the measure of $\mathcal{Q}_i \in \mathbf{Q}$ goes to 0 and the transmission strategy in \mathcal{Q}_i becomes fixed. For example, as the partition progresses, more relay selection variables $\alpha_{s,r}$ become fixed to 0 or 1, and the allowed transmission power for P_s and P_r will be limited to a domain of smaller measure. As $i \rightarrow \infty$, each $\mathcal{Q}_i \in \mathbf{Q}$ contains only fixed relay selection, power allocation and video encoding rate.

Second, as the measure of $\mathcal{Q}_i \in \mathbf{Q}$ goes to 0, the gap between $\text{UP}(\mathcal{Q}_i)$ and $\text{LR}(\mathcal{Q}_i)$ also approaches 0. In Section IV-B, the original problem is relaxed to standard convex problems, whose upper bound $\text{UP}(\mathcal{Q}_i)$ decreases monotonically with decreasing measure of \mathcal{Q}_i . As $i \rightarrow \infty$, the $\text{UP}(\mathcal{Q}_i)$ converges to $\text{LR}(\mathcal{Q}_i)$ with a fixed transmission strategy.

Based on the update criterion of UP_{glb} and LR_{glb} in (33) and (34), the gap between UP_{glb} and LR_{glb} converges to 0 and UP_{glb} and LR_{glb} converge to the globally maximal sum PSNR f^* .